Directional Site Resonances Observed from the 1 October 1987 Whittier Narrows, California Earthquake and the 4 October Aftershock

John E. Vidale
Research Scientist, University of California at Santa Cruz

Ornella Bonamassa
Research Assistant

Heidi Houston
Research Scientist

Abstract

We present evidence that sites often resonate preferentially in a particular compass direction. The 1 October 1987 mainshock and 4 October 1987 aftershock in the Whittier Narrows, California, sequence had very different mechanisms. Nevertheless, at 8 of 11 strong motion stations for which digitized records of both events are available, the direction of strongest shaking in the two events was much more similar than would be expected from their different focal mechanisms. The coincidence of the polarizations from the two events was greatest for the frequencies at peaks in the spectra, suggesting that site amplification and directional resonances are linked. Knowledge of directional site resonances may aid in predicting the directions of damaging earthquake motions.

Introduction

The 1 October 1987 Whittier Narrows California (M_L = 5.9) earthquake and its 4 October aftershock (M_L = 5.3) created an excellent data set of strong motion recordings. These events produced nearly orthogonal radiation patterns. The mainshock had a thrust mechanism and the aftershock had a strike-slip mechanism. Observations from these two sources permit the isolation of site from source effects. Vidale (1989) showed that the 3 to 6 Hz peak accelerations of these two events are modulated by the focal mechanisms. In that study, only peak amplitudes from analog records were utilized. Since eleven records from the aftershock and numerous records from the main shock have now been digitized by the California Strong Motion Instrumentation Program (CSMIP) of the California Division of Mining and Geology, a more broadband quantitative analysis can be done.

Near-receiver geology is an important factor in determining the strength of shaking from an earthquake (Haukkson *et al.*, 1987, Malin *et al.*, 1988). Models of geology that assume homogeneous flat layers can explain some features of observed site amplification (e.g., Joyner *et al.*, 1976). For example, the amplification of 2 sec energy in the lakebed deposits in Mexico City during the 1985 Michoacan earthquake dramatically showed the influence of thin, slow-velocity layers near the Earth's surface (e.g., Campillo *et al.*, 1989).

Patterns of amplification and duration of shaking that require lateral variations in geologic structure have also been documented (Vidale and Helmberger, 1987, 1988), and strong-motion effects of some simple large-scale structures have been investigated (Bard and Gariel, 1986, Kawase and Aki, 1989, Vidale *et al.*, 1985). However, the importance of near-receiver structures more realistic than horizontal layers has not been documented for high-frequency seismic energy. The data analyzed here indicate a need for an increased understanding of the effects of two- and three-dimensional structure near the receiver.

In this paper, to assess the prevalence of frequency- and direction-dependent station resonances, we compare the particle motions of S waves with those predicted from the earthquake focal mechanisms. It is of interest to earthquake engineers whether particular sites have a preferred direction of ground motion in a given frequency range. Initial results from Loma Prieta aftershock recordings (Bonamassa *et al.*, 1990) suggest that such effects occur for more than half the sites investigated, and that the preferred direction does not depend on earthquake location. The results below indicate that directional resonances are a general feature.

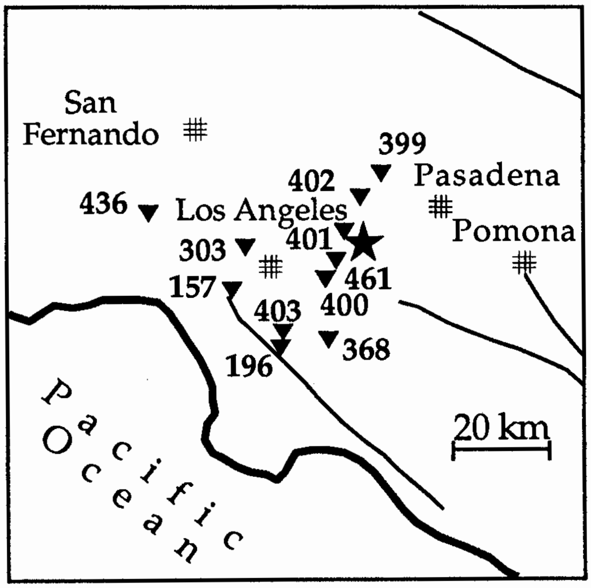

Figure 1. Map showing the location of the 11 CDMG stations. The star indicates the epicentral region of the mainshock and the aftershock, which are separated by only 2 km.

Polarization Analysis for 1 October and 4 October 1987 Whittier Narrows Events

We conduct analysis of the frequency content and polarization characteristics of the Whittier Narrows mainshock and an aftershock to understand the relative contributions of source and site to observed ground motions.

The mainshock hypocenter was located at 14.6 km depth, and the mechanism is a gently dipping thrust (Haukkson and Jones, 1989). Numerous aftershocks filled the volume from 8 to 17 km depth extending about 4 km in all directions horizontally. Bent and Helmberger (1989) analyzed the teleseismic body waves and proposed a double source; their second source is 11 km deep and 5 times larger than the first with a slightly different mechanism. It is important to consider the location and mechanism of the largest patch of moment release to understand the strong ground motions. The double source they propose is best studied with teleseismic body-waves since the strong ground motions are more complicated by the Los Angeles basin near-surface structure. We use the depth and mechanism of their second and largest source to represent the mainshock in this paper. The aftershock that occurred on 4 October 1987 was located 2 km northwest of the mainshock at a depth of 13.3 km, with a strike-slip mechanism on a vertical plane (Haukkson and Jones, 1989).

The 11 stations for which CDMG digitized strong motion records of both the mainshock and the aftershock are shown in Figure 1. The stations range from almost directly above the earthquakes to 50 km distant.

Acceleration spectra for the mainshock and aftershock are shown in Figure 2. The S waves are windowed into 4 sec and 2.5 sec segments for the mainshock and aftershock, respectively, and tapered, and then Fourier transformed. The frequency of the peak acceleration ranges from 1 Hz for station 368 (Downey) to 5-6 Hz for stations 399 (Mt. Wilson). In general, the two spectra from each of the 11 stations are similar, although the mainshock produced a higher level of acceleration.

We processed the Whittier Narrows strong motions as follows: 1) All three components of motion were filtered with a central frequency of 1, 2, 4, 8 and 16 Hz. 2) The particle motion of each filtered record is characterized by its predominant azimuth of polarization (see Vidale, 1986, and Montalbetti and Kanasewich, 1970, for details of polarization analysis). This azimuth of polarization is the equivalent to the direction of the largest excursions in a particle motion diagram. The predominant azimuth of particle motion is compared with the azimuth expected from the source and receiver locations and the focal mechanism of the earthquake.

This procedure is first illustrated in detail for station 157 (Baldwin Hills), then applied to the other ten stations. The S waves from station 157 are shown in Figure 3.

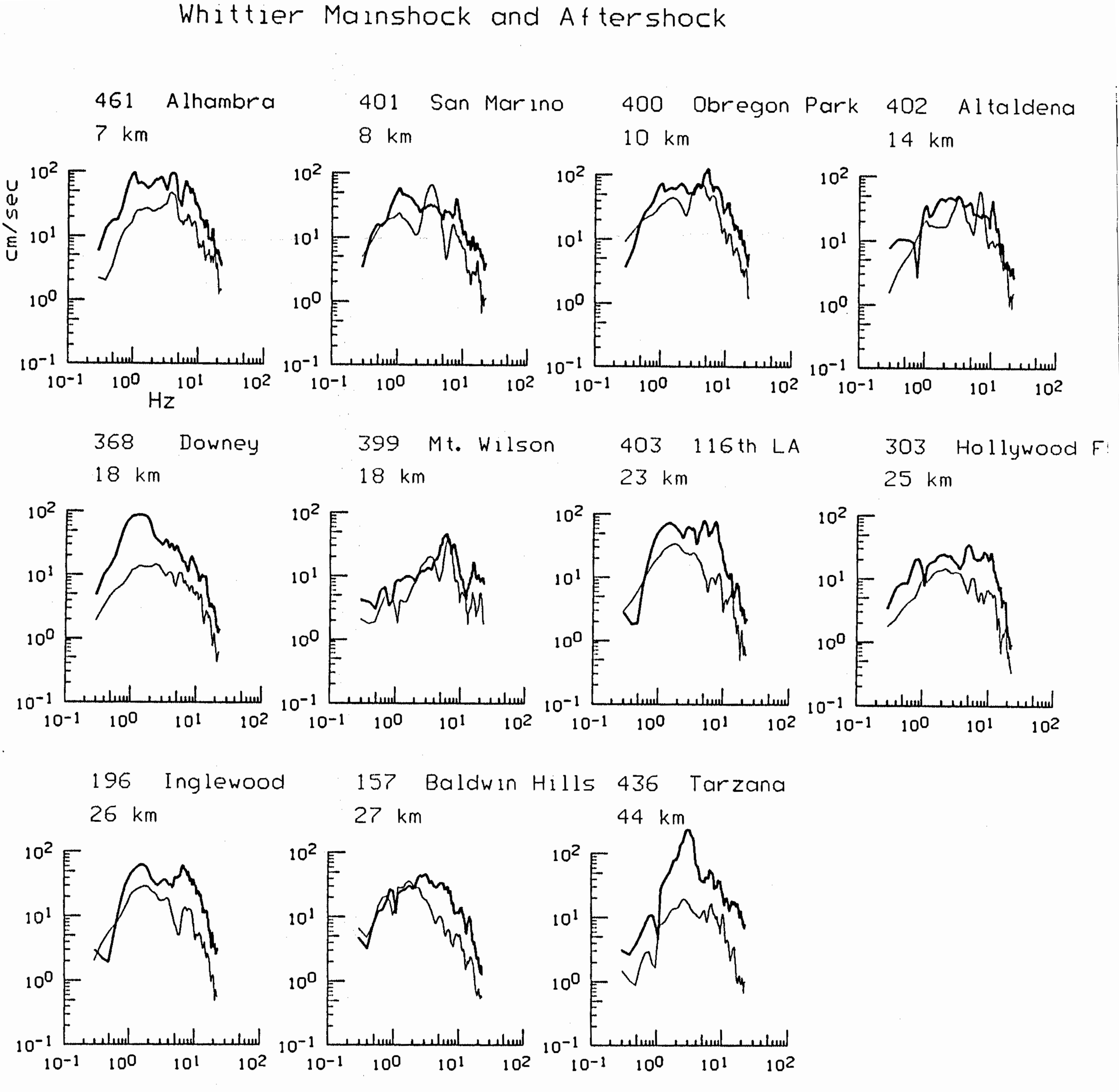

Figure 2. Comparison of acceleration spectra from October 1 mainshock (heavy lines) and October 4 aftershock (light lines) for 11 CSMIP stations. The distance in km from the epicenter is given beneath each station name. The RMS sum of the SH and SV motions is plotted.

Figure 4 shows the particle motions of the passband filtered horizontal motions at station 157, while Figure 5a shows the dominant direction of polarization in each passband. Polarization has the usual two-fold ambiguity, for example, north-south vibration has a direction of either north or south. We therefor plot polarization in the 180° range centered about north.

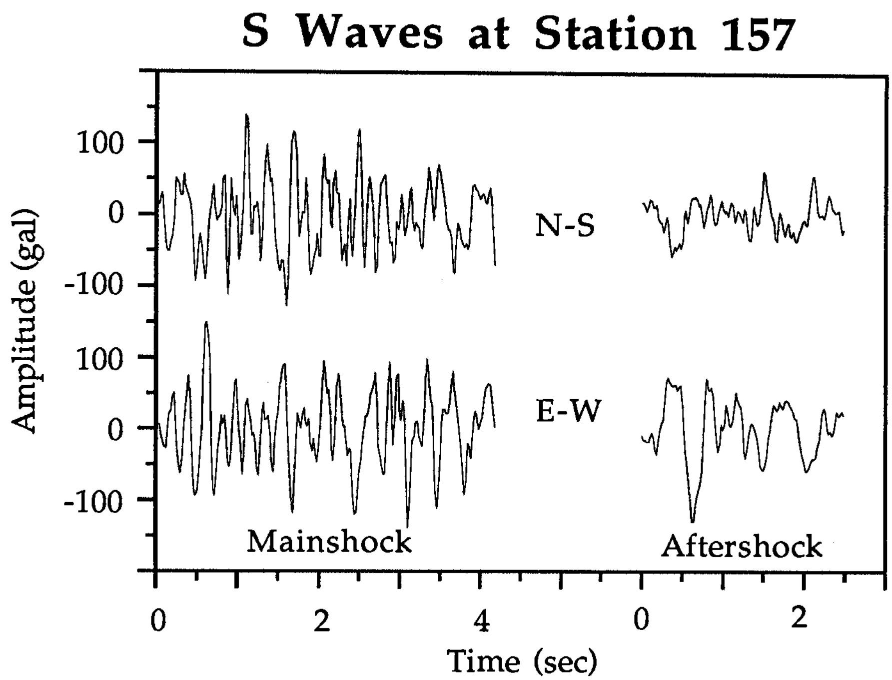

Figure 3. The windowed S waves for the mainshock and aftershock from station 157.

The polarization directions agree between the records for the two events in each pass band, but do not agree particularly well with the directions predicted by the focal mechanisms. The directions of polarization of the broadband signals shown at the right of Figure 5a are similar for the two earthquakes because the azimuths agree fairly well in the 2 and 4 Hz windows where station 157 recorded the strongest accelerations as is apparent in the spectrum in Figure 2. The polarization directions also agree between the two events in other passbands. The directions do not match well between different frequencies, however. These patterns can also be seen in Figure 4, particularly by comparing the 4 Hz and 8 Hz polarizations for the two events.

This pattern suggests that for station 157, 4 Hz shaking tends to be strong in the direction N30W, while 8 Hz shaking is strongest N75E, which is information that may be useful for earthquake engineers. This pattern also suggests that it is not the earthquake source that is controlling the polarization of the S waves at high frequencies. The other ten stations also show similar patterns to varying extents. They are presented in order of increasing station number (i.e., random order).

Particle Motions for the Mainshock at Station 157

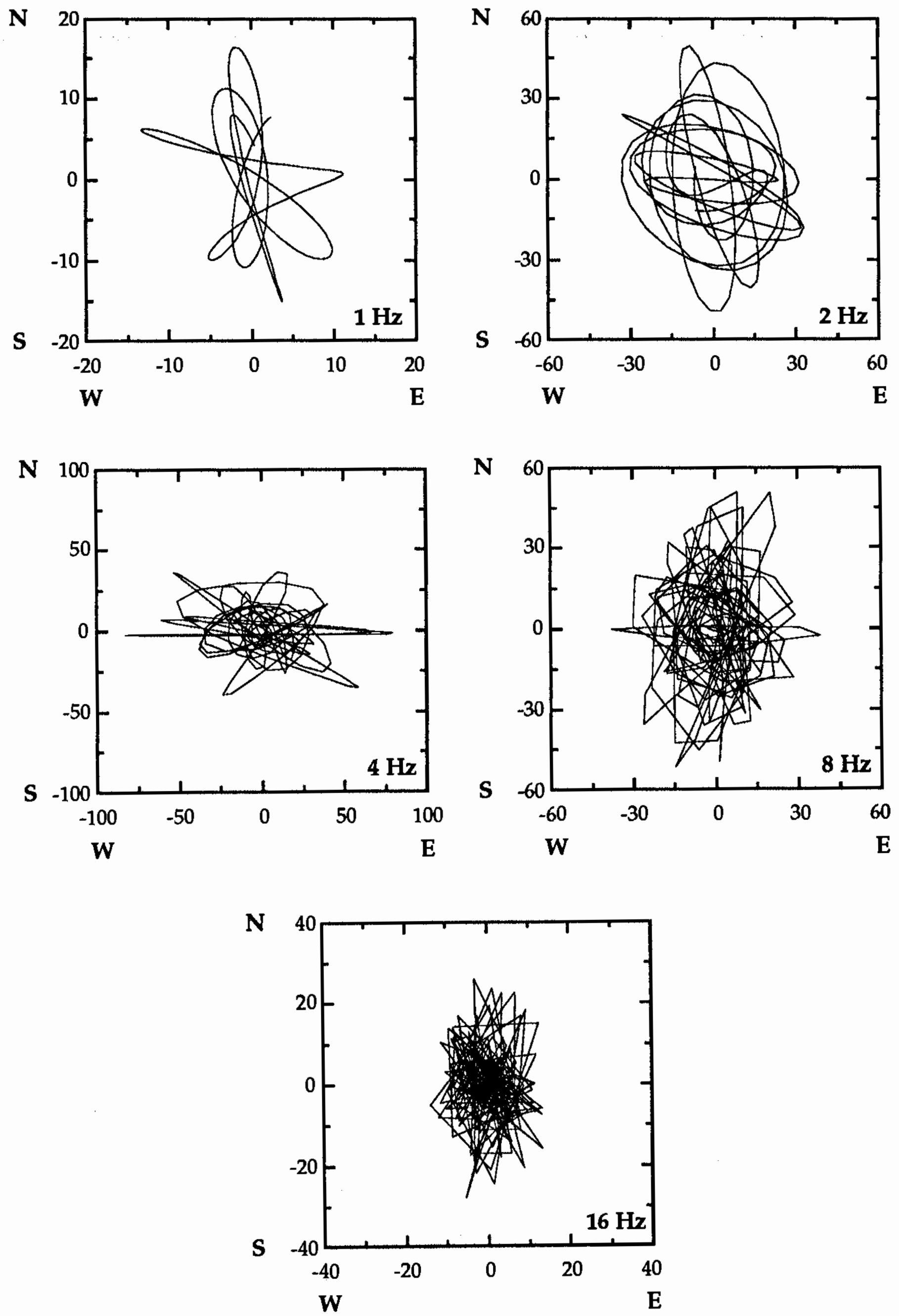

Figure 4a. Particle motion at station 157. Mainshock records bandpassed with 1, 2, 4, 8, and 16 Hz center frequencies.

Particle Motions for the 4 October Aftershock at Station 157

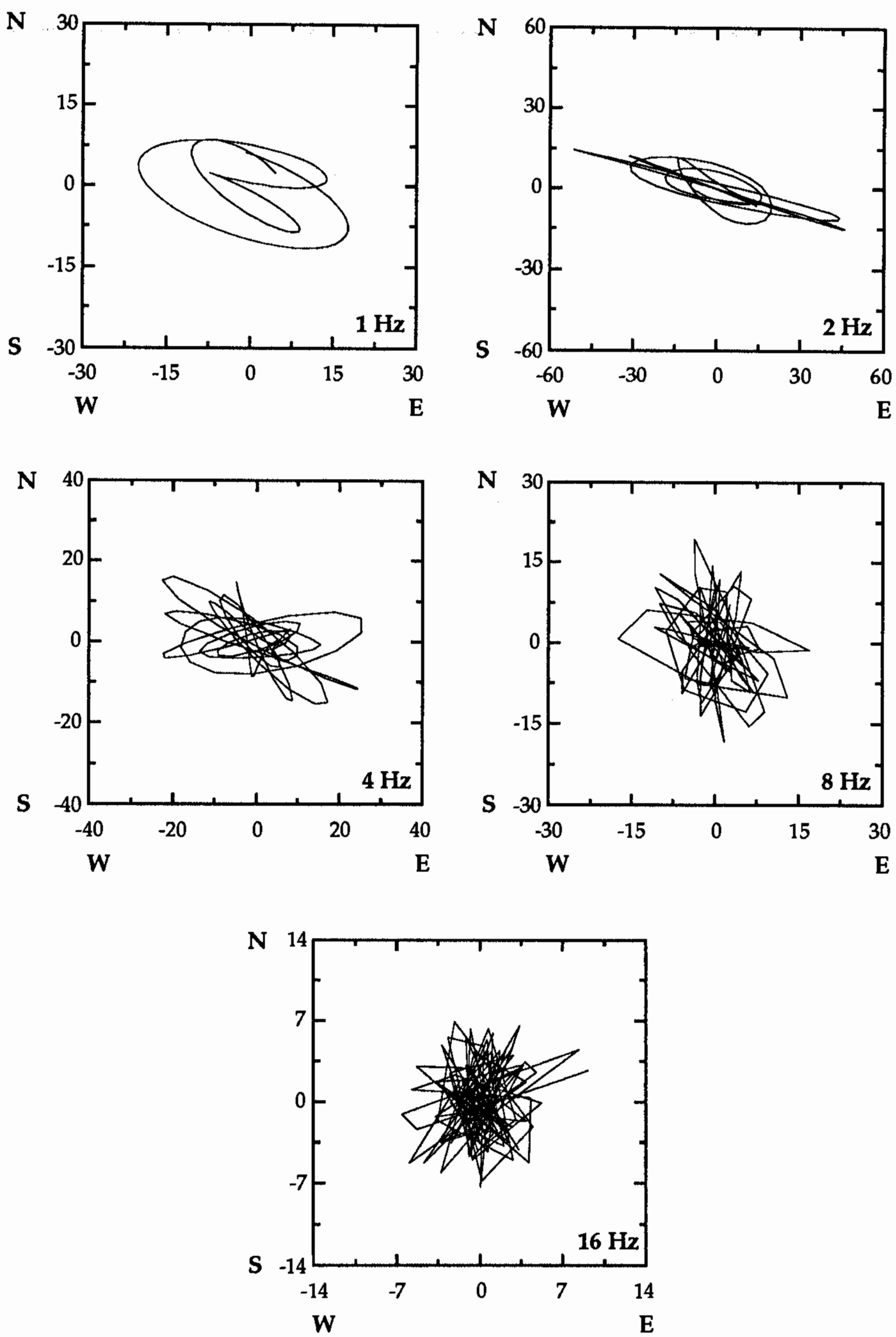

Figure 4b. Particle motion at station 157. Aftershock records bandpassed with 1, 2, 4, 8, and 16 Hz center frequencies.

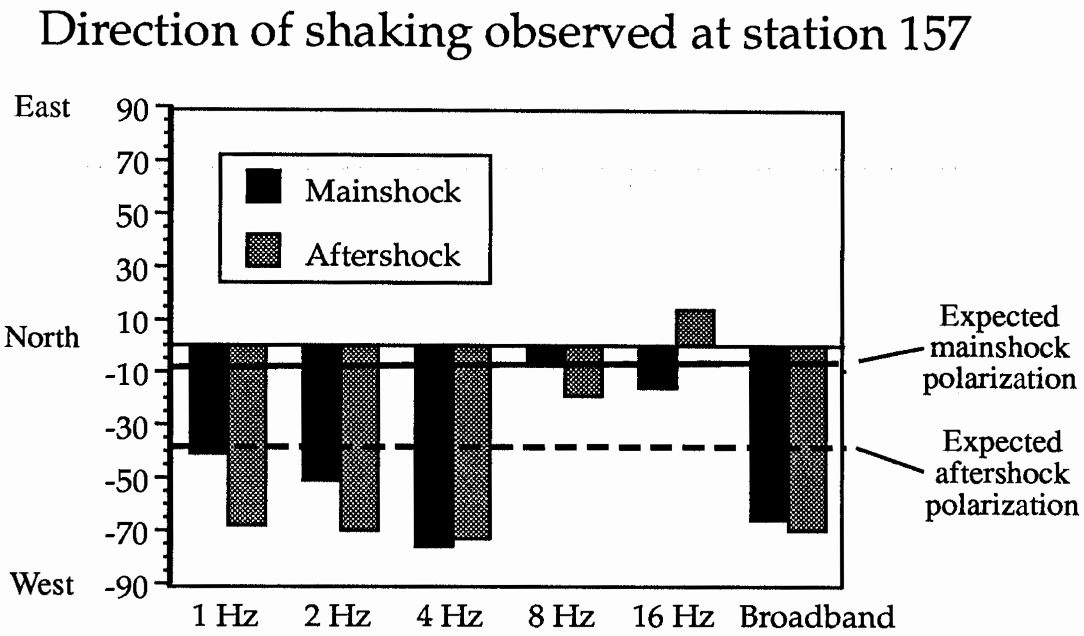

Figure 5a. The primary azimuth of particle motion during the mainshock and aftershock as a function of frequency. The solid and dashed lines indicate the azimuth of polarization expected from the focal mechanisms of the two events, and the bars indicate the polarization measured from the observations. Polarization is measured clockwise from north (north = 0°, northeast = 45°). The polarizations of the mainshock and aftershock are more similar to each other than to the predictions from their respective focal mechanisms.

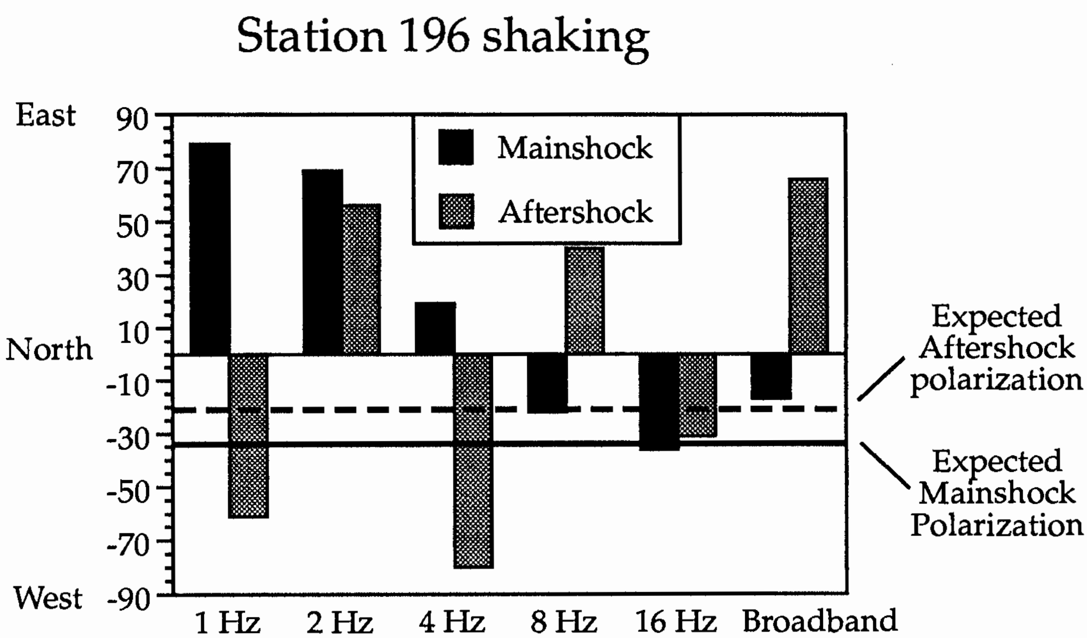

Figure 5b. The azimuth of particle motion of the mainshock and aftershock as a function of frequency for station 196. See caption for Figure 5a.

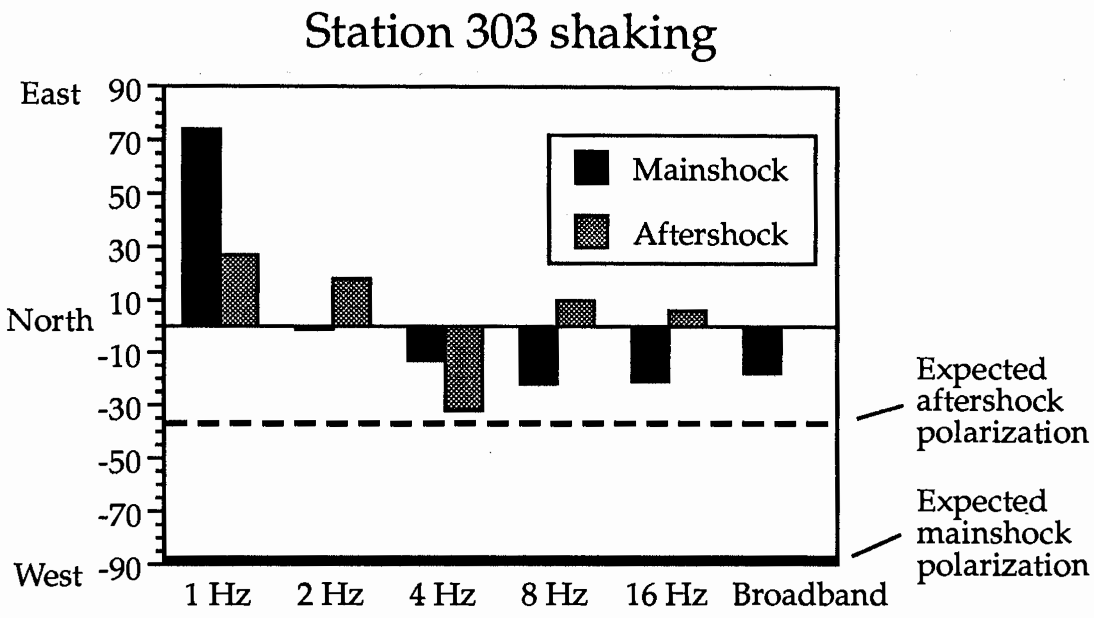

Figure 5c. The azimuth of particle motion of the mainshock and aftershock as a function of frequency for station 303. See caption for Figure 5a.

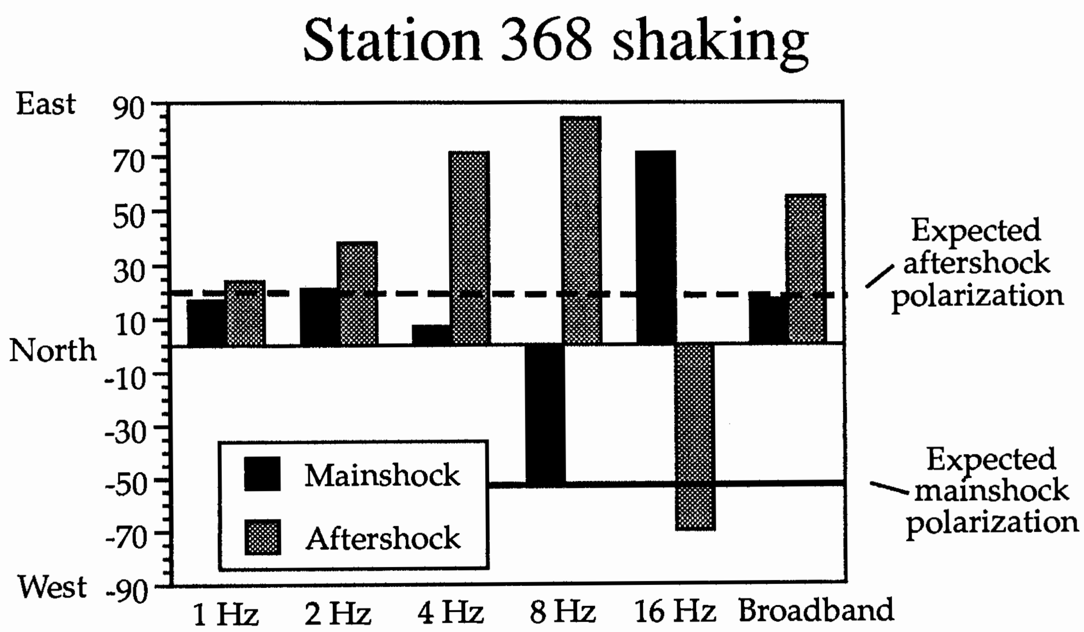

Figure 5d. The azimuth of particle motion of the mainshock and aftershock as a function of frequency for station 368. See caption for Figure 5a.

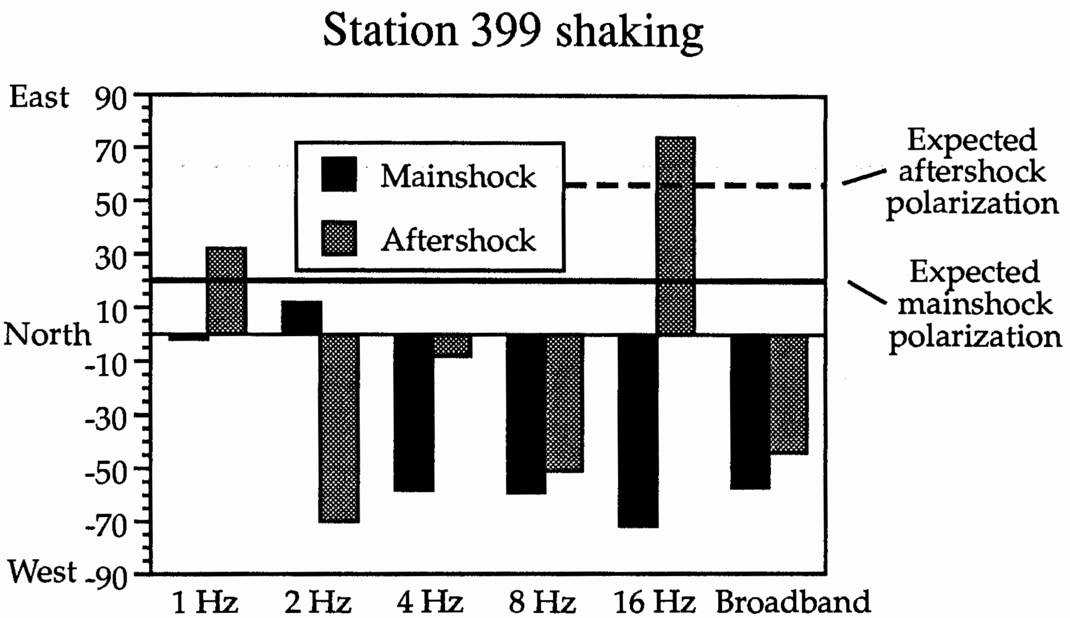

Figure 5e. The azimuth of particle motion of the mainshock and aftershock as a function of frequency for station 399. See caption for Figure 5a.

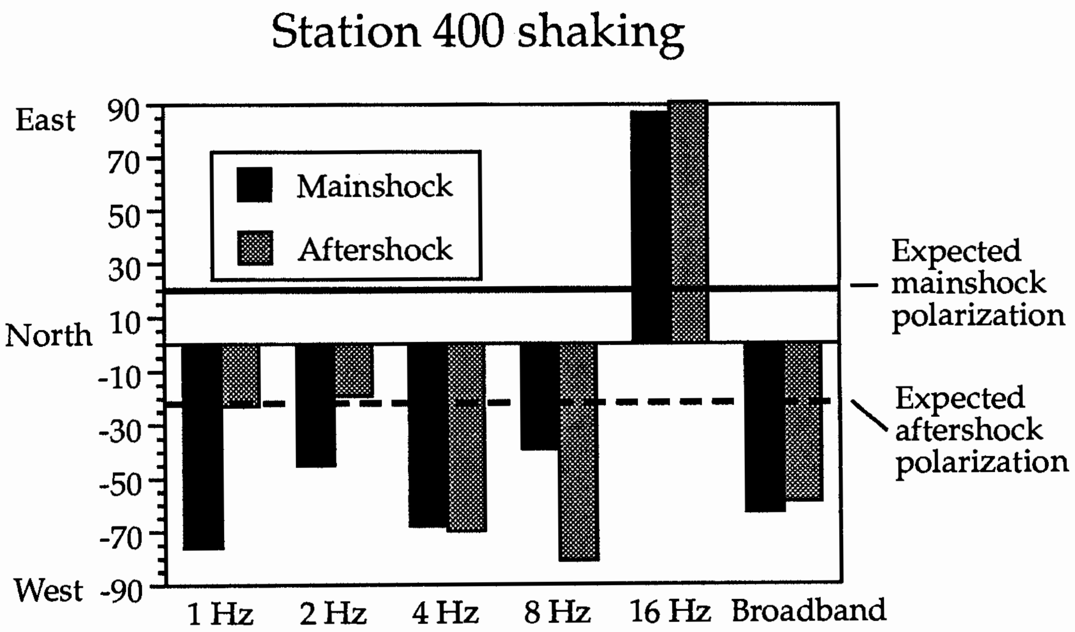

Figure 5f. The azimuth of particle motion of the mainshock and aftershock as a function of frequency for station 400. See caption for Figure 5a.

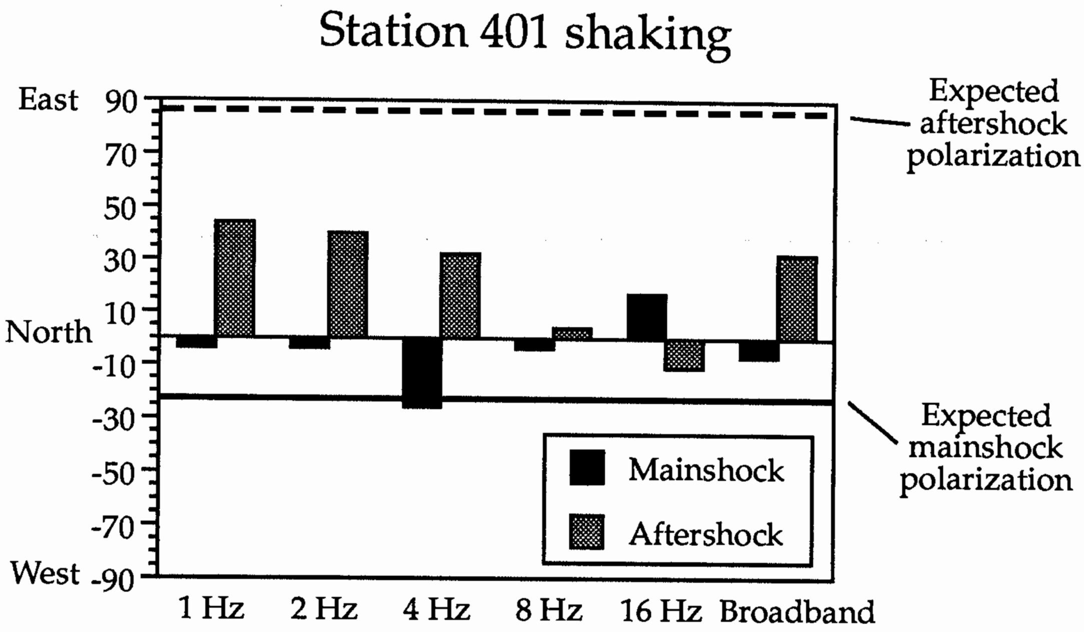

Figure 5g. The azimuth of particle motion of the mainshock and aftershock as a function of frequency for station 401. See caption for Figure 5a.

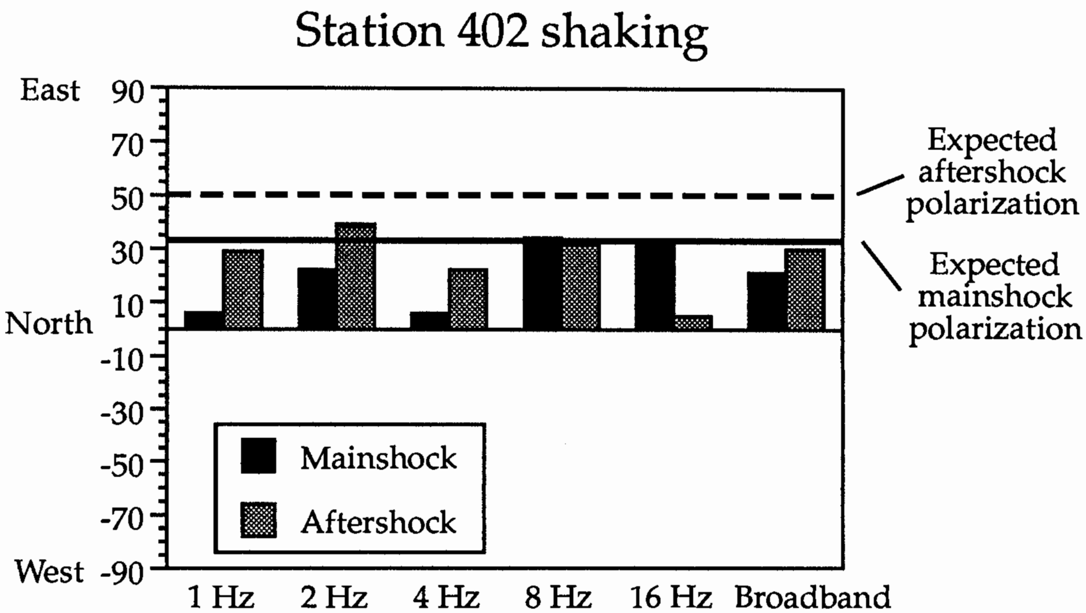

Figure 5h. The azimuth of particle motion of the mainshock and aftershock as a function of frequency for station 402. See caption for Figure 5a.

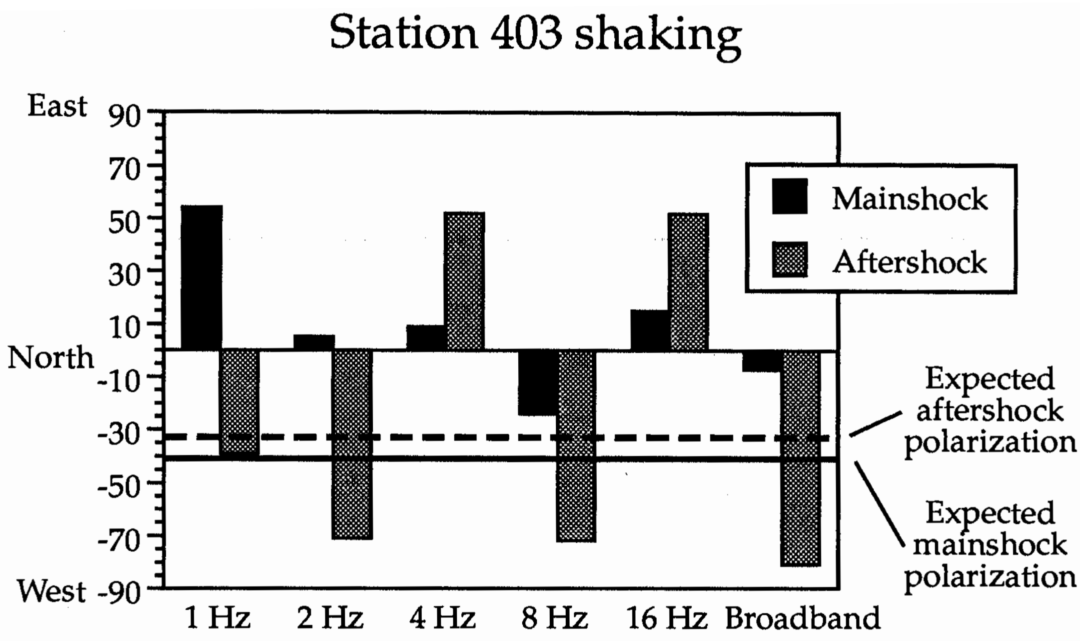

Figure 5i. The azimuth of particle motion of the mainshock and aftershock as a function of frequency for station 403. See caption for Figure 5a.

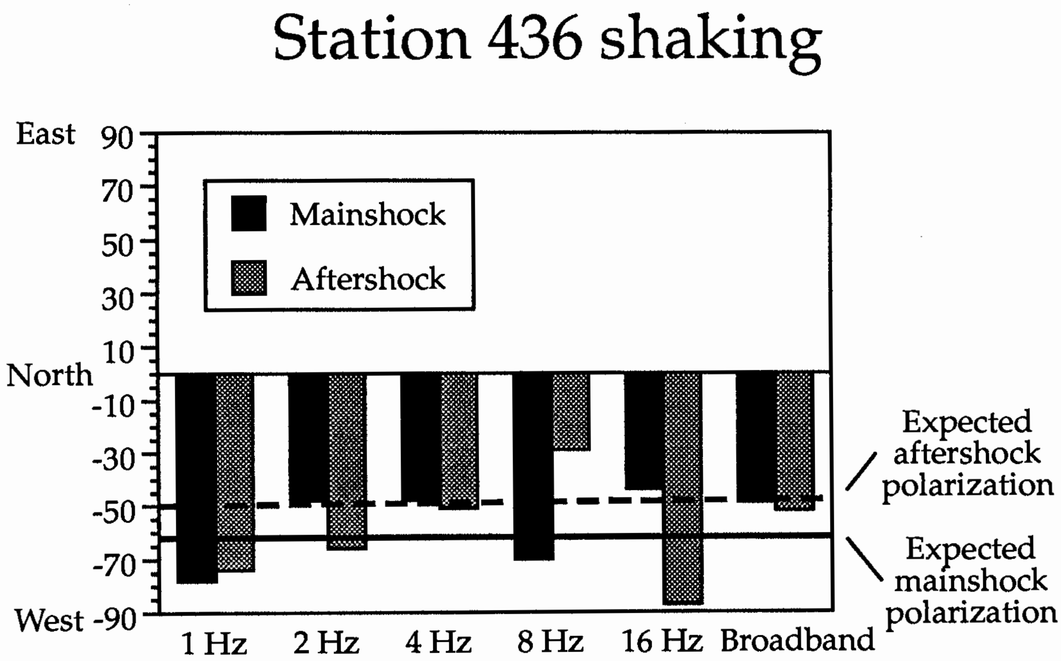

Figure 5j. The azimuth of particle motion of the mainshock and aftershock as a function of frequency for station 436. See caption for Figure 5a.

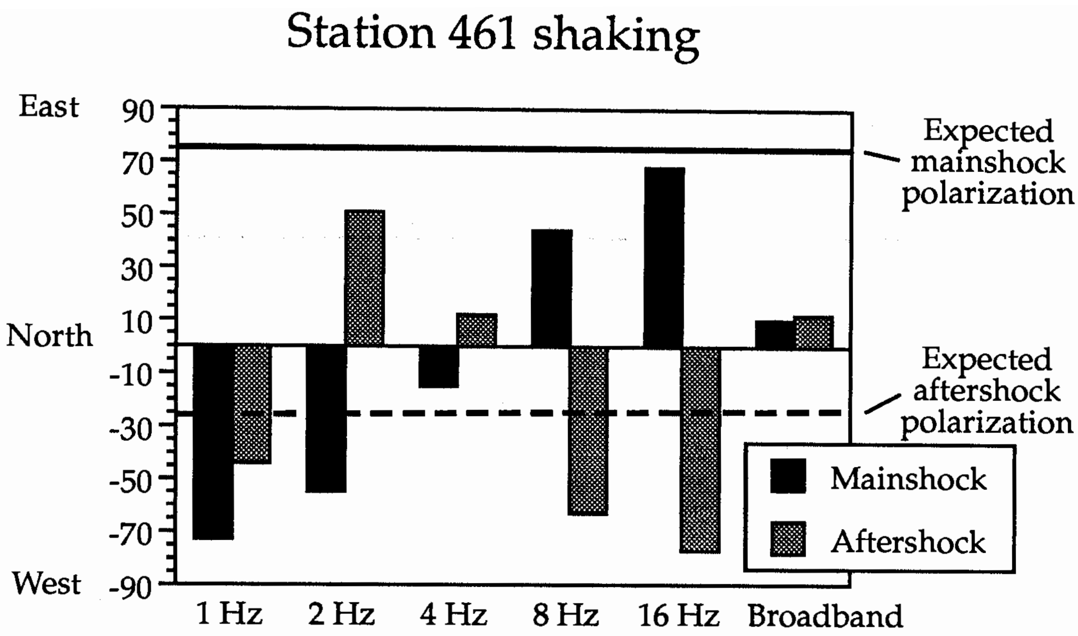

Figure 5k. The azimuth of particle motion of the mainshock and aftershock as a function of frequency for station 461. See caption for Figure 5a.

Station 196 (Inglewood) does not show agreement between the two events in broadband polarization direction, as seen in Figure 5b. Closer examination reveals some evidence for directional site effects, however. The strongest peaks in the two spectra for this station in Figure 2 lie at 2 Hz, and at this frequency the polarization directions agree between the mainshock and the aftershock. The broadband disagreement arises from stronger high frequency energy in the mainshock, but more energy at 1 Hz in the aftershock.

Figure 5c shows good agreement in the broadband polarization for station 303 (Hollywood), despite a large difference in the polarizations predicted by the focal mechanisms. The spectra for this station do not show prominent peaks.

Figure 5d, for station 368 (Downey) shows that the directions of polarization are closer to each other than expected from the focal mechanisms. The 1 Hz passband, which has the largest spectral peak for the mainshock, shows excellent agreement in polarization.

Figure 5e shows the polarization for station 399 (Mt. Wilson). The polarization directions for the two events agree in most pass bands, but again do not agree particularly well with the directions predicted by the focal mechanisms. The azimuths agree fairly well in the 4 and 8 Hz windows where station 399 recorded the strongest accelerations (see Figure 2), and thus again the directions of polarization shown at the right of Figure 5e are very similar for the two earthquakes.

Station 400 (Figure 5f, Obregon Park) has good agreement in polarization direction at 4 Hz, where there is a peak in the spectra. The predicted directions from the focal mechanism are not similar to the observed directions.

Station 401 (Figure 5g, San Marino) does not have good agreement in polarization direction, although even greater disagreement in polarization direction is predicted by the focal mechanism. Different peaks appear in the spectra of the mainshock and aftershock, but no particular pattern is seen.

Station 402 (Figure 5h, Altadena) shows excellent agreement, even better than is predicted from the focal mechanisms. These signals seem coherently polarized at all frequencies, and close to the predicted directions.

Station 403 (Figure 5i, 116th St., Los Angeles) shows poor agreement in polarization direction despite the prediction of good agreement from the focal mechanisms.

Station 436 (Figure 5j, Tarzana) shows excellent agreement in the dominant direction of polarization, perhaps controlled by the sharp peak at 3 Hz. The mainshock and the aftershock are predicted to have a similar direction of polarization. This suggests that the discrepancy between the anomalous amplification seen in Tarzana from the mainshock and the more normal aftershock spectra is *not* due to a difference in the polarization of the incident S waves, which might have resulted in different levels of amplification at Tarzana in the two events.

Station 461 (Figure 5k, Alhambra) shows excellent agreement in broadband polarization direction despite the prediction of orthogonal motion from the focal mechanisms. The spectra are relatively flat.

Figure 6 shows that eight (157, 303, 368, 399, 400, 402, 436, 461) of the eleven stations have similar polarizations for the mainshock and the aftershock. This suggests that a majority of the stations may have a characteristic direction of polarization, which does not change from event to event.

Previous work (Vidale, 1989) on the Whittier Narrows sequence suggests that the focal mechanism controls peak acceleration at a site, but the data presented here indicate that in many cases, the azimuth of polarization of the motion in the range 1-16 Hz depends on the site. In addition, in several cases, including stations 157, 196, 368, 399, 400, 436, the most similarity between the mainshock and aftershock polarizations is in the pass band where spectral peaks appear, suggesting that the geologic features that enhance amplitudes in a particular frequency band also have a preferred direction of particle motion. The 11 stations span a wide range of surficial geology from hard rock to soft sediment, summarized in Table 1, suggesting that these directional resonances are probably a common feature.

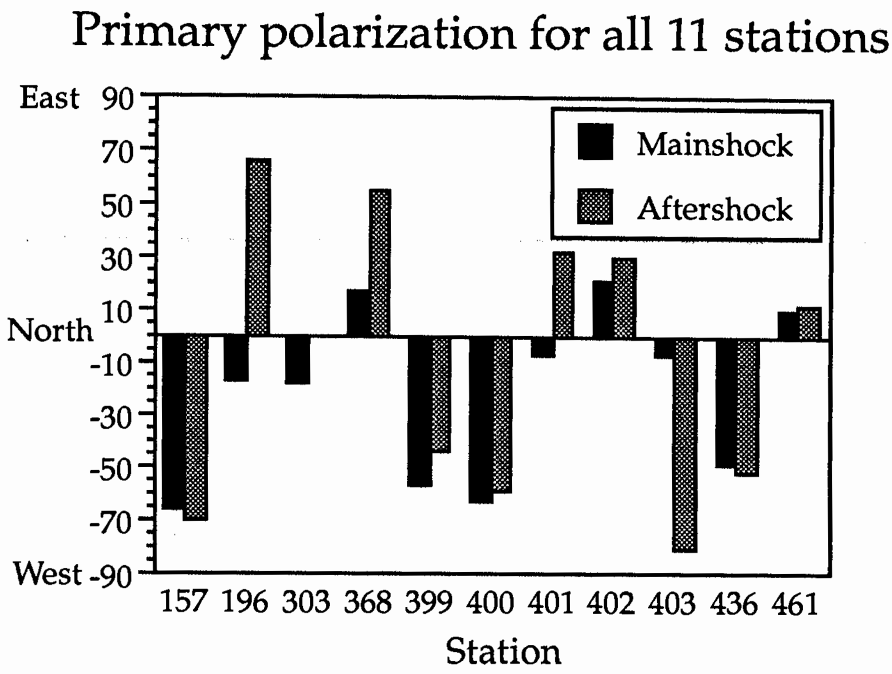

Figure 6. Observed directions of the strongest polarization of the broadband signal for acceleration records from the Whittier Narrows mainshock and aftershock for 11 stations. The predicted polarizations from the first-motion focal mechanisms do not agree as well. Polarizations are measured clockwise from north.

The present study provides results that complement those of Bonamassa *et al.* (1990). Bonamassa *et al.* (1990) find that S waves from 11 aftershocks of the Loma Prieta earthquake recorded at a dense 6-station 3-component array in the Santa Cruz mountains show directional resonances. The resonances vary within the array on a scale of 25 meters, but persist for a given station for a range of earthquake locations and expected S-wave polarizations. The rapid variation across the array suggests very near-surface structure is causing the resonances. The present study has higher quality stations that are situated in a wider range of surficial geologies, suggesting that these resonances are a common occurrence.

The most likely explanation for these azimuthal patterns is that particle motion in one compass direction is amplified compared to the motion in other directions. The specific geological structures that cause this amplification are not yet known. Surface topography seems unlikely, as Buchbinder and Haddon (1990) estimate only small S-wave azimuthal anomalies due to topography. The most likely structures are strong lateral variation in the S-wave velocity in the top 10's of meters, where velocity can be very low.

Conclusions

Three-component seismic recordings for 8 of 11 stations of the Whittier Narrows earthquake sequence show that in the frequency range from 1 to 16 Hertz, there is a preferred direction of ground motion, which we term "directional resonance" that does not depend on the polarization of the shear waves expected from the focal mechanism. The study of Bonamassa et al. (1990) also finds directional resonances and suggests that the preferred direction also does not depend on the earthquake location. The coincidence of the polarizations from the two events was greatest for the frequencies at peaks in the spectra, suggesting that site amplification and directional resonances are linked. This study has focused on S waves since they carry the largest amplitude motions in the near-field and are of interest to earthquake engineers.

These preliminary conclusions drawn from good data for various sites in the Los Angeles area suggest that in-depth analysis of the processes that control directional resonances is necessary. Earthquake engineers as well as seismologists will benefit from knowledge of the strength of the characteristic resonance at a site and the area over which it is coherent.

Acknowledgements

This work was supported by the California Department of Conservation, Division of Mines and Geology, Strong Motion Instrumentation Program under contract number OSMS 8-8068. The contents of this paper were developed under a contract from the California Department of Conservation, Division of Mines and Geology, Strong Motion Instrumentation Program. However, those contents do not necessarily represent the policy of the agency, and you should not assume endorsement by the State Government. Support for this work has been provided in part by a grant from the W.M. Keck Foundation, and the Institute of Tectonics, University of California, Santa Cruz.

References

Bard, P.-Y., J.C. Gariel, 1986. The seismic response of two-dimensional sedimentary deposits with large vertical velocity gradients, *Bull. Seism. Soc. Am.*, **76**, 343-360.

Bent, A.L., and D.V. Helmberger, 1989. Source complexity of the 1 October 1987 Whittier Narrows Earthquake, *J. Geophys. Res.*, **94**, 9548-9556.

Blakeslee, S.N., 1989. Studies in near-surface, crustal and fault-zone attenuation: borehole analysis of Parkfield earthquakes, *Ph.D. Thesis*, University of California at Santa Barbara.

Bonamassa, O., J.E. Vidale, S.Y. Schwartz, 1990. Observations of directional site resonances from the Loma Prieta earthquake sequence, in preparation for *Bull. Seism. Soc. Am...*

Buchbinder, G.G.R., and R.A.W. Haddon, 1990. Azimuthal anomalies of short period P-wave arrivals from Nahanni aftershocks, N.W.T., Canada and effects of surface topography, *Bull. Seism. Soc. Am.*, in press.

Campillo, M., J.C. Gariel, K. Aki, and F.J. Sánchez-Sesma, 1989. Destructive strong ground motion in Mexico City: source path and site effects during the great 1985 Michoacán earthquake, *Bull. Seism. Soc. Am.*, **79**, 1718-1734.

Haukkson, E., and L. Jones, (1989). The 1987 Whittier Narrows Earthquake sequence in Los Angeles, southern California, seismological and tectonic analysis, *J. Geophys. Res.*, **94**, 9569-9590.

Haukkson, E., T.-L. Teng, T.L. Henyey, 1987. Results from a 1500 m deep, three-level downhole seismometer array, *Bull. Seism. Soc. Am.*, **77**, 1883-1904.

Joyner, W.B., R.E. Warrick, and A.A. Oliver, III, 1976. Analysis of seismograms from a downhole array in sediments near San Francisco Bay, *Bull. Seism. Soc. Am.*, **66**, 937-958.

Kanamori, H., 1979. A semi-empirical approach to prediction of long-period ground motions from great earthquakes, *Bull. Seism. Soc. Am.*, **69**, 1645-1670.

Kawase, H. and K. Aki, 1989. A study on the response of a soft basin for incident S, P, and Rayleigh waves with special reference to the long duration observed in Mexico City, *Bull. Seism. Soc. Am.*, **79**, 1361-1382.

Malin, P.E., J.A. Waller, R.D. Borcherdt, E. Cranswick, E.G. Jensen, and N. Van Schaak, 1988. Vertical seismic profiling of Oroville microearthquakes: velocity spectra and particle motion as a function of depth, *Bull. Seism. Soc. Am.*, **78**, 401-420.

Montalbetti, J.R., and E.R. Kanasewich, 1970. Enhancement of teleseismic body phases with a polarization filter, *Geophys. J. R. astr. Soc.*, **21**, 119-129.

Vidale, J.E., 1986. Complex polarization analysis of particle motion, *Bull. Seism. Soc. Am.*, **76**, 1393-1406.

Vidale, J.E., 1989. Influence of focal mechanism on peak accelerations for the Whittier Narrows, Ca. earthquake and an aftershock, *J. Geophys. Res.*, **94**, 9607-9615.

Vidale, J.E., and D.V. Helmberger, 1987. Path effects in strong motion seismology, chapter in volume of *Methods of Computational Physics*, Bruce Bolt, ed., 267-319.

Vidale, J.E., and D.V. Helmberger, 1988. Elastic finite-difference modeling of the 1971 San Fernando, Ca. earthquake, *Bull. Seism. Soc. Am.*, **78**, 122-142.

Table 1 : Stations co-ordinates and geology

Station	Latitude	Longitude	Directional Resonance	Surficial Geology
157	34.01	118.36	Yes	Fill over shale, sandstone
196	33.90	118.28	No	Terrace deposits
303	34.09	118.34	Yes	Alluvium (130 m) over sandstone, shale
368	33.92	118.17	Yes	Deep alluvium
399	34.22	118.06	Yes	Quartz Diorite
400	34.04	118.18	Yes	Alluvium
401	34.11	118.13	No	Alluvium
402	34.18	118.10	Yes	Alluvium
403	33.93	118.26	No	Terrace deposits
436	34.16	118.53	Yes	Shallow alluvium (10 m) over sandstone, shale
461	34.07	118.15	Yes	Alluvium